Phase and amplitude variations of optically induced spin transients

Martin Rosatzin, Dieter Suter, Wulfhard Lange,* and Jürgen Mlynek

Institute of Quantum Electronics, Swiss Federal Institute of Technology (ETH) Zürich, CH-8093 Zürich, Switzerland

Received November 13, 1989; accepted February 1, 1990

We report detailed studies of freely evolving Zeeman coherence (Zeeman quantum beats) observed after optically pumping a gas of Na atoms and suddenly turning off the light field. This Zeeman coherence corresponds to a macroscopic magnetization that precesses in an external magnetic field; it is detected with a cw optical probe beam by using polarization-selective detection of the transmitted light. The amplitude and the phase of the signal show a pronounced variation with laser intensity, laser detuning, and the strength of the magnetic field. This dependence was measured on the $3s\ ^2S_{1/2}$ ground state of sodium, using the D_1 line for optical excitation and detection. The experimental data are compared with theoretical predictions based on a Bloch-type equation of motion for an optically driven spin system in a $J = 1/2$ ground state.

1. INTRODUCTION

Laser-induced coherent transients are a powerful tool for sublevel spectroscopy of gases, liquids, and solids. In this context, quantum-beat experiments have been used extensively for high-resolution spectroscopy of neighboring excited atomic and molecular states. In these experiments, a coherent superposition of the neighboring states is prepared with a light pulse that is in general resonant with both optical transitions. This superposition state is then allowed to precess freely, and the interference between the two probability amplitudes is observed as a time-dependent oscillation in the fluorescence signal.[1] For the theoretical analysis of such quantum-beat experiments in the excited state it is usually assumed that the intensity of the driving light field is well below the saturation level so that the resulting signal is linear in the laser intensity. While this is typically the case with conventional light sources, the use of pulsed lasers can lead to conditions in which higher-order effects such as stimulated emission and a shift of energy levels can become important.

A theory of saturation effects of laser-induced quantum beats was developed previously by Silverman *et al.*[2] In their approach they not only included the limit of impact excitation by a short laser pulse but also analyzed the case in which the length of the excitation pulse is no longer negligible in comparison with the precession period of the superposition state. At low laser power, such an extended excitation time leads to relatively small quantum-beat signals. Simply, this effect can be explained in terms of coherence packets, which are generated during the pumping process. After being generated they start acquiring a phase, owing to precession under the influence of the atomic Hamiltonian; packets that are generated at different times therefore acquire different phases and interfere distructively with one another. However, Silverman *et al.* found that the amplitude of the beats can become substantial even for long excitation pulses if the intensity of the pump pulse is raised well above the saturation level, an effect that they called "saturation regeneration of quantum beats." Until now these theoretical predictions had not been verified experimentally.

On the other hand, it is well known that superpositions of atomic substates can also be induced in atomic ground states in a coherent optical Raman process. These coherences between ground-state sublevels can easily be detected, e.g., by an optical probe beam, giving rise to so-called quantum beats in forward scattering.[3–5] Since the relaxation time of ground-state coherences is generally much longer than the lifetime of excited states, studies of substate coherences can be performed on a convenient time scale (of the order of microseconds). Furthermore, other conditions being equal, the laser power required to saturate a transition between two degenerate ground-state sublevels is much smaller than that required for the saturation of the excited-state sublevels; the ratio of the saturation intensities is equal to the ratio of the corresponding relaxation times.[6] At the low intensity levels required for an experiment in the ground state, excitation pulses of arbitrary length can be derived from single-mode cw lasers by electro-optic or acousto-optic means; moreover, the narrow linewidth of the laser permits detailed studies of the quantum-beat signals as a function of optical resonance detuning. If the substates are Zeeman sublevels, the splitting between them can be controlled experimentally and the signal measured as a function of the sublevel splitting.

Here we use this experimental approach to study the amplitude and phase variations of optically induced Zeeman coherences in the $3s\ ^2S_{1/2}$ ground state of atomic sodium. Instead of using the term quantum beats, we prefer to call the observed transients free-induction-decay (FID) signals, in analogy to magnetic-resonance experiments using radio-frequency fields.[4,7] A long pulse of circularly polarized laser light is applied close to the D_1 resonance line to create the ground-state superposition, and the subsequent FID of the spin coherence is observed with a cw optical probe beam. Since the excita-

0740-3224/90/071231-08$02.00

tion pulse is derived from a cw laser and can be made arbitrarily long, we do not need to work in the impact approximation but can drive the system until it reaches an equilibrium state.

The observed FID signal is that of a freely precessing system, i.e. the oscillation frequency of the FID is not broadened or shifted by the optical pulse. The amplitude and the phase of the freely oscillating transient, however, are determined by the preparation and show a pronounced dependence on laser intensity, optical resonance detuning, and sublevel splitting.[8] In this respect our research extends previous quantum-beat studies[1] and optical pumping experiments involving coherence phenomena in atomic ground states.[9] The observed behavior of the sublevel FID reported here can be explained quantitatively with a simple theory based on a Bloch-type equation for the evolution of an optically driven $J = 1/2$ system. In Section 2 this theoretical approach is presented in more detail.

2. OPTICALLY PREPARED SUBLEVEL COHERENCES

The basic idea behind our experiment is illustrated graphically in Fig. 1. Figure 1(a) is a schematic representation of the atomic level system considered; Fig. 1(b) summarizes the experimental setup. The ground and excited states of our model system are both $J = 1/2$ states. We have chosen the propagation direction of the laser beam as the quantization axis. If the pump beam (solid lines) is right-circularly polarized, it couples to the transition between the states $|1\rangle$ and $|4\rangle$. If the laser intensity is well

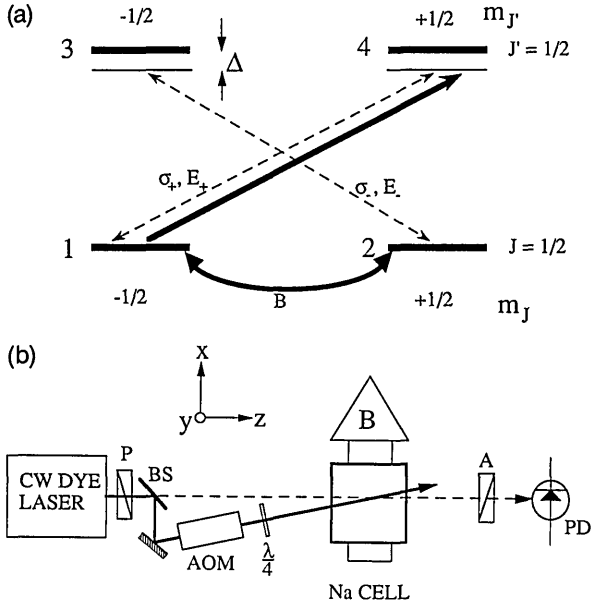

Fig. 1. (a) Schematic representation of the $J = 1/2$–$J' = 1/2$ system coupled to the optical fields. The quantization axis is parallel to the propagation direction of the laser beam so that the atomic substates remain degenerate, even in the presence of a transverse magnetic field, B. In this representation, the magnetic field induces transitions between the substates, indicated by the curved line. (b) Schematic representation of the experimental setup: P, polarizer; BS, beam splitter; AOM, acousto-optic modulator; $\lambda/4$, retardation plate; B, magnetic field; A, polarization analyzer; PD, photodiode.

below the saturation intensity for the optical transition, we can neglect the population of the excited state; the primary effect of the laser field is then the depletion of the $m_J = -1/2$ ground state. The resulting population difference between the two magnetic substates of the atomic ground state leads to different absorption and dispersion for right- and left-circularly polarized light, which can be detected by another laser beam. For this probe beam (dashed lines) it is advantageous to choose linearly polarized light, which can be thought of as a superposition of equal amounts of left- and right-circularly polarized light. The circularly polarized components act as probes for the two transitions with $m_{J'} - m_J = \pm 1$. Our detection scheme separates these components and measures the different strengths of the two transitions and thereby the population difference between the two ground-state sublevels.

The magnetic moment associated with the transition between the Zeeman substates also couples to an external magnetic field B. In our experiment we apply a static magnetic field perpendicular to the laser beam. If we temporarily change the direction of quantization, the connection between our experiment and the usual quantum-beat experiments becomes apparent. In a coordinate system in which the quantization axis lies along the direction of the magnetic field, the atomic levels are split by the Zeeman interaction.[10] If the homogeneous width of the optical transition or the spectral width of the laser pulse is larger than the Zeeman splitting, the laser radiation is resonant with both transitions from the ground to the excited state, and a Raman-type process can occur that leads to coherence between the two ground-state levels.

In our experiment the optical pumping of the sample is continued until transient effects have disappeared and a steady-state polarization of the atomic ground state is established. The size of this polarization and its orientation in space depend on the intensity and the resonance detuning of the laser, the strength of the magnetic field, and the ground-state relaxation rate. Quantum mechanically, this equilibration process corresponds to a decay of the off-diagonal elements of the density operator in the eigenbase of the Hamiltonian of the system including the coupling to the laser radiation. When the optical pump beam is suddenly switched off, the Hamiltonian of the system changes such that the density operator has off-diagonal elements in the new eigenbase. The evolution of these density operator elements corresponds to a precession of the magnetization around the magnetic field. The polarization-selective detection measures the magnetization component parallel to the laser beam; the precession appears therefore as an oscillation that is damped by the ground-state relaxation rate. The amplitude and the phase of this FID depend on the size and the orientation of the steady-state polarization established during the optical pumping process.

For a quantitative analysis, it is useful to introduce the vector $\mathbf{m}$ for the ground-state polarization as[11]

$$\mathbf{m} = [\rho_{12} + \rho_{21}, -i(\rho_{12} - \rho_{21}), \rho_{22} - \rho_{11}]. \qquad (1)$$

The longitudinal component m_z of the magnetization, i.e., the component parallel to the laser beam, is given by the difference of the populations of the ground-state sub-

levels, while the transverse components m_x and m_y correspond to the real and imaginary parts, respectively, of the coherence between them. Equation (1) does not merely represent a parameterization of the density operator; the vector $\mathbf{m}$ is also directly proportional to the macroscopic magnetization vector. In our coordinate system the z component is oriented along the laser beam, while the x component lies along the direction of the magnetic field.

As is shown elsewhere,[11,12] the dynamics of the system coupled to the radiation field can be simplified considerably by disregarding the optical coherences and the population of the excited state. This is possible if the optical coherences decay fast compared with the dynamics of the ground state and if the laser intensity is well below the saturation intensity of the optical transition. Experimentally, these conditions can be realized by adding buffer gas to the sample cell, leading to a pressure broadening of the homogeneous optical resonance line. Under these conditions, the dynamics of our model system occurs exclusively in the two ground-state levels and can be described by the magnetization vector $\mathbf{m}$.

The effect of the pump laser can be parameterized by the pump rate

$$P_+ = \frac{|\beta_+|^2}{\Gamma_2(1 + \bar{\Delta}^2)}, \tag{2}$$

where $\beta_+ = \mu_e E_+/2\hbar$ represents the optical Rabi frequency and $\bar{\Delta} = \Delta/\Gamma_2$ denotes the detuning Δ of the laser frequency from exact optical resonance, normalized to the half-width at half-height Γ_2 of the optical resonance line; positive $\bar{\Delta}$ corresponds to blue detuning. μ_e is the electric dipole moment of the transition $|1\rangle \leftrightarrow |4\rangle$, and E_+ describes the electric field amplitude of the circularly polarized pump pulse. The optical field has a threefold effect on the dynamics of the spin system: it generates ground-state polarization in the direction of propagation, causes relaxation of the existing magnetization, and, if the laser frequency is detuned from exact resonance ($\Delta \neq 0$), it shifts the energy of the state to which the radiation field is coupled. For the spin dynamics, this level shift, often called the light shift, has the same effect as a magnetic field along the direction of the laser beam.[13]

The equation of motion of the system under the influence of laser and magnetic field is[11,12]

$$\dot{\mathbf{m}} = \mathbf{\Omega} \times \mathbf{m} - \gamma_{\text{eff}}\mathbf{m} + \mathbf{P}, \tag{3}$$

with

$$\mathbf{\Omega} = (\Omega_L, 0, \bar{\Delta}P_+), \qquad \Omega_L = \frac{\mu_B g B}{\hbar}, \qquad \mathbf{P} = (0, 0, P_+),$$

$$\gamma_{\text{eff}} = \gamma + P_+. \tag{4}$$

Here μ_B denotes Bohr's magneton, g is the Landé factor, and B is the magnetic field. The effective relaxation rate γ_{eff} is given by the sum of the relaxation rate γ due to diffusion of the atoms out of the laser beam and the relaxation due to coherence-destroying optical pumping. The orientation of the fields $\mathbf{\Omega}_L$, $\bar{\Delta}\mathbf{P}$, and $\mathbf{\Omega} = (\Omega_L, 0, \bar{\Delta}P_+)$ is shown graphically in Fig. 2. As we pointed out above, we are interested in the case of long-pulse excitation in which the duration of the pulse is long compared with the relaxation time γ_{eff}^{-1}, in which case the magnetization is determined by the stationary solution of the equation of motion

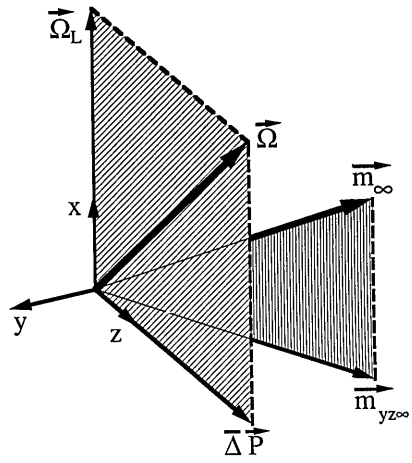

Fig. 2. Representation of the magnetic field $\mathbf{\Omega}_L$ and the pseudofield $\bar{\Delta}\mathbf{P}$ due to the light-shift effect, together with the equilibrium magnetization $\mathbf{m}_\infty$ and its projection into the yz plane $\mathbf{m}_{yz\infty}$. For details see text.

$$\mathbf{m}_\infty = \frac{P_+}{\gamma_{\text{eff}}(\Omega_L^2 + \bar{\Delta}^2 P_+^2 + \gamma_{\text{eff}}^2)} \times (\bar{\Delta}P_+\Omega_L, -\gamma_{\text{eff}}\Omega_L, \bar{\Delta}^2 P_+^2 + \gamma_{\text{eff}}^2). \tag{5}$$

The relative orientation of this equilibrium magnetization is also shown in Fig. 2. If the pump beam is suddenly switched off, the magnetization generated during the pulse is no longer in equilibrium but starts to precess around the magnetic field that lies along the x axis. The equilibrium magnetization during the pulse is therefore also the initial condition for the FID. We choose the end of the pump pulse as the origin of our time axis, so that the evolution of the magnetization can be written as

$$\mathbf{m}(t) = [m_{x\infty}, -A\sin(\Omega_L t + \phi), A\cos(\Omega_L t + \phi)]e^{-\gamma t}. \tag{6}$$

Here $m_x(0) = m_{x\infty}$ is the x component of the stationary magnetization generated by the pump pulse. Since this component is parallel to the magnetic field, it has no oscillatory time dependence but merely decays with the relaxation rate γ. Amplitude A and phase ϕ of the orthogonal component precessing in the yz plane are given as

$$A = [m_y(0)^2 + m_z(0)^2]^{1/2} = \frac{P^+}{\gamma_{\text{eff}}} \frac{[\gamma_{\text{eff}}^2\Omega_L^2 + (\bar{\Delta}^2 P_+^2 + \gamma_{\text{eff}}^2)^2]^{1/2}}{\Omega_L^2 + \bar{\Delta}^2 P_+^2 + \gamma_{\text{eff}}^2}, \tag{7}$$

$$\tan\phi = -\frac{m_y(0)}{m_z(0)} = \frac{\gamma_{\text{eff}}\Omega_L}{\bar{\Delta}^2 P_+^2 + \gamma_{\text{eff}}^2}. \tag{8}$$

The instantaneous z component of the magnetization is directly proportional to the detected signal[12]; the amplitude and the phase of the FID signal are therefore determined by Eqs. (7) and (8). This is shown graphically in Fig. 3: on the left-hand side the projection of the magnetization into the yz plane is shown; the arrow represents the magnetization vector immediately after the end of the excitation pulse, and the dashed spiral shows the subse-

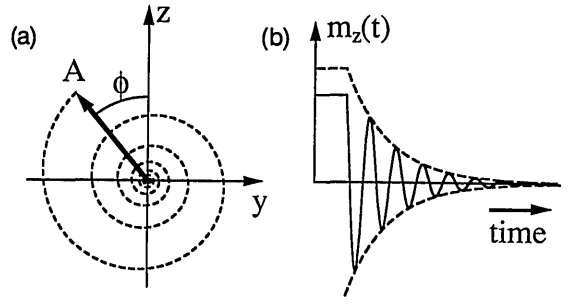

Fig. 3. (a) Projection of the magnetization vector $\mathbf{m}$ into the yz plane. The arrow represents the stationary magnetization and the dashed spiral the evolution after the end of the optical excitation pulse. Amplitude A and phase ϕ of the FID are given by the polar coordinates of the thick arrow. (b) z component of the magnetization as a function of time (solid curve) and the FID envelope $\pm A \exp(-\gamma t)$ (dashed curves).

quent evolution due to Larmor precession and damping. The solid curve on the right-hand side displays the z component of the magnetization vector as a function of time; it is therefore directly proportional to the FID signal. The dashed curves represent the envelope of the FID, $\pm Ae^{-\gamma t}$, which is given by the instantaneous length of the precessing magnetization component $\mathbf{m}_{yz}$.

Equations (7) and (8) show that the amplitude and the phase of the FID signal depend strongly on the laser intensity and on the optical resonance detuning. This dependence can be seen more easily in the limit where the optical pumping rate is large compared with the relaxation due to diffusion, $P_+ \gg \gamma$. This condition is usually fulfilled as long as the irradiation frequency is near resonance. We then have

$$A = \frac{p\sqrt{1+p^2}}{1+p^2+\bar{\Delta}^2}, \tag{7'}$$

$$\tan\phi = 1/p, \tag{8'}$$

where $p = |\beta_+|^2/\Gamma_2\Omega_L$ is the ratio of the on-resonance optical pumping rate to the Larmor frequency. In the limit considered here, the phase of the FID signal depends only on this dimensionless parameter, while the amplitude has a Lorentzian dependence on the resonance detuning. It reaches a maximum of $p/\sqrt{1+p^2}$ on resonance and falls off to half of this value at $\bar{\Delta} = \pm\sqrt{1+p^2}$.

The variation of the equilibrium magnetization during the pulse, i.e., the initial condition for the FID, as a function of laser intensity is illustrated in Fig. 4. The projection into the yz plane $\mathbf{m}_{yz}(0)$ is shown as a function of laser intensity for two different resonance detunings of the exciting laser pulse. For high enough laser intensity, $P_+ \gg \Omega_L$, the equilibrium magnetization is oriented almost parallel to the z axis ($\phi \sim 0$), and the amplitude can reach values near unity. This corresponds to a complete polarization of the ground state. If the laser intensity is decreased, the amplitude of the ground-state polarization decreases, and the projection of the magnetization vector tilts toward the y axis. For the observed signal, this corresponds to an increase of the phase toward 90°. The arrows indicate the position of the magnetization vector at a laser intensity of $p = 2$. The two vectors differ only in their length, not in their orientation, as predicted by Eq. (8').

3. EXPERIMENTAL RESULTS

Our experiments were performed on the Zeeman sublevels of the $^2S_{1/2}$ ground state of atomic sodium. The D_1 line ($\lambda = 589.6$ nm) was used for optical excitation. The details of the experimental apparatus are described elsewhere.[12] A schematic representation of the experimental setup is shown in Fig. 1(b). The sodium-cell temperature was 180°C, and 210 mbars of argon was added as a buffer gas, causing a pressure broadening of the optical resonance line to a half-width at half-maximum of 2.1 GHz. The small-signal absorption at the line center was 20%. From the absorption profile we calculated a particle density of 4.5×10^9 cm^{-3}; the total number of atoms in our probe volume was thus some 7×10^7. The intensity of the pump beam was changed by adjusting an attenuator in the beam, while the intensity of the probe beam was kept constant. The diameter of both beams (full width at half-maximum) was between 0.3 and 0.7 mm, depending on the experiment.

In order to get good detection sensitivity over a large detuning range, we measured the magnetization through its influence on the difference of the dispersion of right- and left-circularly polarized light, in contrast to the experiments described before,[12] in which differential absorption was measured. The experimental realization of the polarization-selective detection is shown in Fig. 5. The probe beam was split into two partial beams behind the sample, both of which were passed through polarizers whose axis was rotated by 45° with respect to the polarization of the probe beam before the sample. Each of the two partial beams was focused onto a photodiode; the difference of the two photocurrents was then amplified and recorded with a digital storage oscilloscope. The resulting signal is

$$\Delta I = I_0 \exp(-\alpha_0 l)\sin(2m_z d_0). \tag{9}$$

Since this is an odd function of the magnetization, the zero-order term as well as the second-order term vanishes, and the linear term is usually a good approximation of the signal,

$$\Delta I_1 = m_z d_0 I_0 \exp(-\alpha_0 l). \tag{10}$$

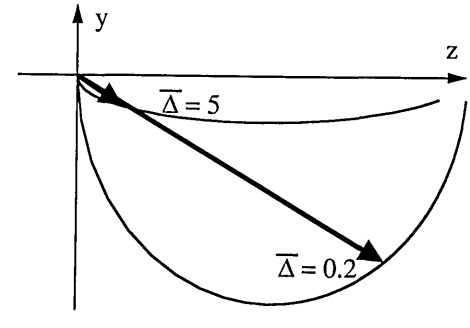

Fig. 4. Equilibrium magnetization $\mathbf{m}_{yz}(0)$ as a function of optical pump rate for two different detunings. The optical pump rate $|\beta_+|^2/\Gamma_2$ runs from 0 to 2×10^7 sec^{-1}. The arrows represent the values for $\chi^2/\Gamma_2 = 2 \times 10^6$ sec^{-1} in each curve. The other parameters are $\Omega_L/2\pi = 159$ kHz and $\gamma = 10^4$ sec^{-1}.

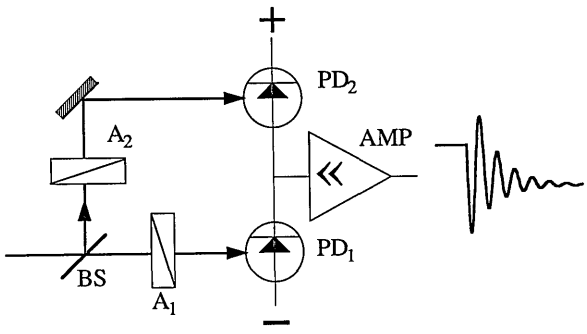

Fig. 5. Experimental realization of the polarization selective detection: BS, beam splitter; A's, polarization analyzers; PD's, photodiodes; AMP, amplifier.

Here d_0 and α_0 represent the frequency-dependent dispersion and absorption coefficients, respectively, of the unpolarized medium, I_0 is the laser intensity, and l is the interaction length. The detected signal is thus proportional to the z component of the magnetization; the detection sensitivity is given by the intensity of the probe beam multiplied by the dispersion of the unpolarized medium; it vanishes therefore on resonance, reaches a maximum near $\Delta = \pm\Gamma_2$, and falls off as $1/\Delta$ for large detunings.

If the excitation pulse length is comparable with the period of the initial transient, the amplitude and the phase of the FID are both functions of the pulse length.[14] Here we consider only the limit of long excitation pulses, where an equilibrium ground-state polarization is reached before the pump beam is switched off. Details of the initial transient are given elsewhere.[12]

In order to measure the phase of the precession signal, it is essential to have a well-defined origin of the time axis. Since this reference point is determined by the time at which the pump beam is turned off, rectangular pulses should be used. In our experiment we use an acousto-optic modulator to generate the pulses. The rise and fall times of our pulses were 200 and 400 nsec, respectively, short compared with the Larmor period of 1–10 μsec.

Figure 6 shows two examples of experimental signals at two different intensities of the pump laser, together with the time-dependent laser amplitude. It is obvious that in both cases an equilibrium ground-state polarization is reached before the pump beam is turned off. The different amplitudes of the FID signals are apparent from the different scale of the two traces; for the upper trace, the phase ϕ of the FID, as defined by Eq. (6), is close to 0, whereas it is almost 90° in the lower trace. As can be seen from Fig. 3, the phase of the FID is determined by the orientation of the magnetization vector in the yz plane. At high laser intensity the evolution of the magnetization is determined mainly by the optical irradiation, and the equilibrium magnetization is oriented close to the z axis; in the FID signal this results in a phase close to 0. At lower intensities the equilibrium magnetization becomes smaller and tilts toward the y axis (see Fig. 4); the phase of the FID increases accordingly toward 90°. In the case of the lower trace in Fig. 6, the equilibrium magnetization appears to be oriented almost parallel to the y axis.

Measurements of signal amplitude and phase as a function of the laser intensity at three different Larmor frequencies Ω_L are shown in Fig. 7 together with the theoretically predicted dependence as derived from Eqs. (7) and (8). The resonance detuning of the laser was set to $\Delta/2\pi = 10.5$ GHz ($\bar{\Delta} = 5$) for all measurements. The overall scaling factor for the FID amplitudes and the scaling factor for the conversion of laser power to optical pump rates were used as adjustable parameters for the calculation of the theoretical curves. At low intensities the FID amplitude increases almost linearly with the optical pump rate. As the pump rate exceeds the Larmor frequency the system becomes almost fully polarized, and the signal saturates. The phase of the FID signal decreases simultaneously toward 0.

The measured variation of the ground-state magnetization with the optical detuning is shown in Fig. 8 together with the theoretical prediction. The measurements were performed with a constant pump laser power of 15 mW. The upper half of the figure again shows the amplitude of the FID, and the lower half shows the phase. Since the detection sensitivity depends on the resonance detuning of the laser, the z component of the magnetization as determined by Eq. (7) has to be multiplied by the dispersion of the unpolarized medium and the transmission coefficient. As a consequence, the signal vanishes on resonance, as shown in the top trace. For larger detunings the signal falls off owing to the decrease in the optical pumping rate as well as to the decreasing detection sensitivity. Over the detuning range measured, the phase was almost independent of detuning, in agreement with Eq. (8′).

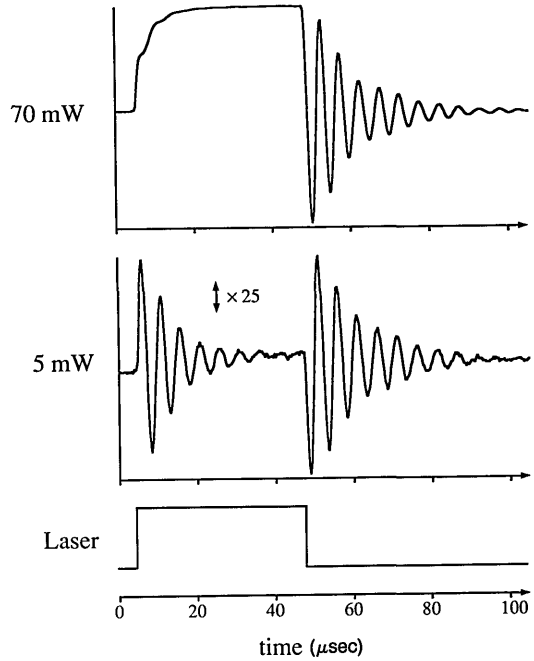

Fig. 6. FID signals measured with two different laser powers. Note the different scales. Experimental parameters: $\Omega_L/2\pi = 200$ kHz, $\Delta/2\pi = 10.5$ GHz. The lowest trace indicates the amplitude of the laser pulse.

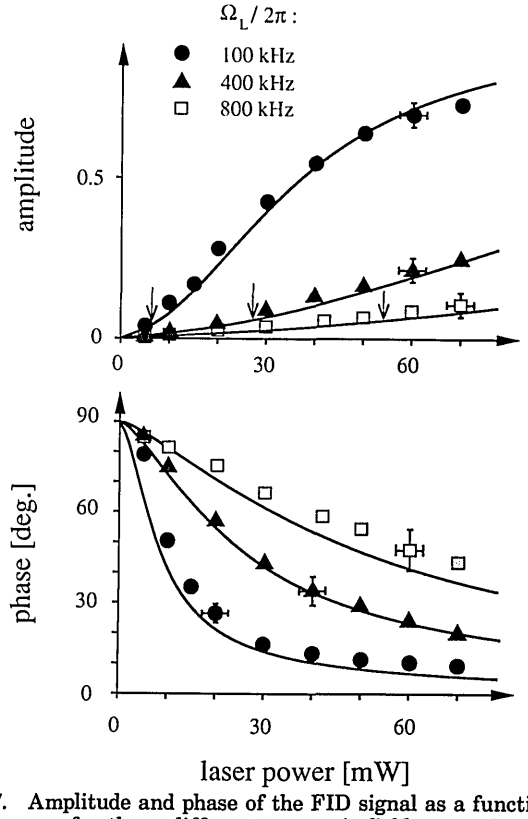

Fig. 7. Amplitude and phase of the FID signal as a function of laser power for three different magnetic-field strengths. The experimental data points are compared with the theoretical prediction. The optical detuning was set to $\Delta/2\pi = 10.5$ GHz, and the decay rate was $\gamma = 12 \times 10^3$ sec^{-1}. The amplitude scale represents relative ground-state polarization, and the arrows indicate where $p = |\beta_+|^2/\Gamma_2\Omega_L = 1$ for each curve.

The theoretical calculations were all done for ideal conditions, in which the angle between laser beam and magnetic field is exactly 90° and the pump beam is circularly polarized. We have taken care to provide conditions as close to these as possible in the experiments. In order to get an idea of the effects of some unavoidable nonidealities, we have calculated the FID signal under conditions of a misaligned magnetic field and an elliptically polarized pump laser. While the effect on the amplitude of the FID is in both cases relatively small, the phase is affected more strongly. Under the influence of a longitudinal magnetic field, the dependence of the FID on the optical detuning becomes asymmetric. The effect of an elliptical polarization of the pump beam is a decrease of amplitude and phase near resonance. While we have largely eliminated these effects, another imperfection was not eliminated: the theoretical calculations assumed that the laser field was homogeneous throughout the sample, whereas the experiments were performed with two beams with approximately Gaussian profiles.

4. DISCUSSION

The theoretical and experimental results presented here show the dependence of amplitude and phase of optically prepared sublevel coherences on laser intensity, laser detuning, and sublevel splitting. These results can be compared with the theoretical work of Silverman *et al.*[2] in which they calculated the dependence of quantum-beat signals on the laser intensity for the limit of long excitation pulses. They found that, in the limit of weak optical pumping, the amplitude of the quantum-beat signal is given by the Fourier transform of the pulse shape, evaluated at the frequency that corresponds to the level splitting in the excited state. If the pulse is longer than the precession period, the beat amplitudes are therefore relatively small; this can be interpreted as destructive interference between coherence packets that were created at different times by the optical pumping process and have therefore acquired different phases during their free evolution. However, if the laser intensity is raised far above the saturation intensity, the amplitude of the quantum-beat signal increases, an effect that they called "saturation regeneration of quantum beats."

These results were obtained by numerical integration of the equations of motion; since no analytical solution was available, they could give only a qualitative analysis of this effect. In their view, "the effect of saturation is to slow down the coherence precession rate, and thereby prevent the destructive interference from washing out the beats during the passage of the pulse." However, according to their equation of motion, the atomic system should reach an equilibrium state in a time of order T_p (in their notation the inverse of the optical pumping rate); a saturation parameter of $S = 5$ (in their notation), e.g., implies that the system has, in a sense, progressed more than 99% toward its equilibrium state. A further increase of the saturation parameter should therefore not lead to any significant changes of the equilibrium polarization.

In our case, the equations of motion can be solved analytically. The FID signal observed in our experiment is

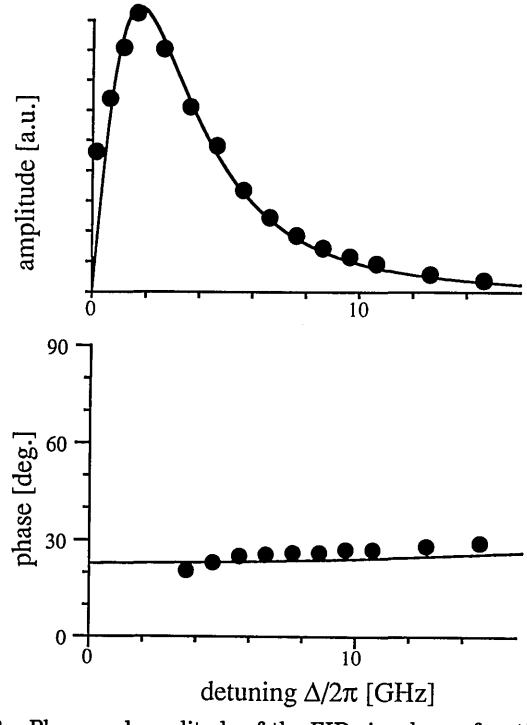

Fig. 8. Phase and amplitude of the FID signal as a function of optical detuning. The experimental data points are compared with the theoretical prediction. The parameters used for the calculation were $\chi^2/\Gamma_2 = 1.5 \times 10^6$ sec^{-1}, $\gamma = 8.5 \times 10^3$ sec^{-1}, and $\Omega_L/2\pi = 102$ kHz.

in principle identical to the signal that they calculate, except that in our case the sublevels contributing to the superposition state are sublevels of the electronic ground state. Another difference is that in our experiment we use a narrow-band laser, whereas they assumed broadband excitation. However, a narrow-band laser irradiating a broad transition is basically equivalent to broadband irradiation of a narrow resonance line. In either case, the important condition is that the radiation be resonant with both transitions, which is always satisfied as long as the spectral width (laser linewidth or homogeneous optical width) is large compared with the level splitting.

In order to compare our results with those of Silverman *et al.*, we specialize to the conditions considered by them. The analogous case is described by our formulas (7) and (8) in the limit of very long relaxation times, $\gamma \to 0$, and on-resonance irradiation, $\Delta = 0$. The FID amplitude is then

$$A = \frac{p}{\sqrt{1 + p^2}} = \frac{P_+}{\sqrt{\Omega_L^2 + P_+^2}}. \tag{11}$$

The condition for strong optical pumping is therefore $P_+ \gg \Omega_L$, under which the system becomes fully polarized ($A \to 1$). It is important to realize that this condition defines the equilibrium position of the system and that this equilibrium is reached in a time of order P_+^{-1}. The physical interpretation of this condition is that the time evolution of the system becomes dominated by the optical pumping and the precession due to the sublevel splitting vanishes in first order. In addition, the optical pumping leads to relaxation of the system, which means that the memory of the coherence extends only over a time of the order of P_+^{-1}. No matter how long the system is pumped, the coherence present in the system was generated during the last P_+^{-1} seconds and can therefore not be dephased by more than Ω_L/P_+. For strong pumping this phase can be made arbitrarily small. The average phase acquired by the different coherence packets during the pumping process becomes directly visible in our experiment as the phase of the FID signal. According to the arguments developed above, the FID amplitude should go to zero as the phase approaches 90°. Inspection of Fig. 7 shows that this is clearly the case.

This explanation is partly consistent with that of Silverman *et al.* However, the equilibrium position of the system changes as the pulse amplitude is lowered. If the variation of the pulse amplitude is slow enough, the system follows adiabatically and remains in equilibrium with the external fields. When the pulse amplitude reaches zero, the equilibrium magnetization vanishes also, and the beat amplitude goes to zero. Even if the optical pumping at the pulse maximum is very large ($p \gg 1$), the signal vanishes if the pulse is not switched off fast enough. In this case, the coherence that was generated during the pumping process is destroyed again, mainly while the pump rate is lowered through the region of $p \sim 1$.

In their numerical calculations Silverman *et al.* assumed a Gaussian pulse shape. While a relatively small saturation parameter of, e.g., $p = 2$ is sufficient to polarize the system to 90%, this polarization is partly lost while the Gaussian pulse is turned off. In order to compensate for this effect, they used extremely strong pulses. A simple calculation shows that the time during which the laser amplitude is in the critical region of, say, $p = 2$ to $p = 0.2$ is decreased by a factor of 4 if the maximum pulse amplitude is raised from $p = 2$ to $p = 4000$. The system is therefore left with much less time to lose the coherence generated by the optical pumping during the pulse. The necessity for strong pulses arises therefore not from the need for strong pumping but from the need to switch off the pulse fast enough. In our experiment, we use relatively low laser intensities, but the nearly rectangular pulse shape guarantees that the switching off of the pulse occurs nonadiabatically and the full polarization is observed in the FID signal.

In addition to the dependence on the laser amplitude and the sublevel splitting, we have also investigated the dependence of the FID on the resonance detuning of the laser. In this case, the effect of the light shift becomes important. It has a dispersionlike dependence on the detuning and therefore falls off more slowly ($\sim\Delta^{-1}$) than the optical pumping rate ($\sim\Delta^{-2}$). Since the virtual field produced by the light shift is parallel to the direction of the laser beam, the magnetization generated by the optical pumping process is no longer forced to precess around the direction of the magnetic field and can accumulate over longer pumping times. As a result the amplitude of the FID falls off more slowly as a function of resonance detuning than would be expected by considering only the optical pumping.

Variations of the amplitude and the phase of the FID signal as a function of the strength of the exciting field are known not only in optically pumped systems but also in other coherently excited systems such as spin systems excited with pulses of radio-frequency radiation.[15] The reason for these variations is basically a variation of the direction of the effective field $\mathbf{\Omega}$. In the case of rf spectroscopy, two components contribute to this effective field: one component is given by the resonance detuning of the rf field, the other by the rf field strength. In the optical case discussed here, one component of the effective field is given by the Larmor frequency, while the other is determined by the light shift that depends on the resonance detuning of the laser. However, in the optical case not only is the magnetization rotated by the effective field but in addition magnetization is generated by the optical pumping. This is basically the reason why we can observe a magnetization even for prolonged laser irradiation, while in the case of rf excitation the pulse length must be kept short in order to avoid decay of the magnetization.

Although the FID signals that we observe here are excited with laser pulses, they should not be confounded with optical FID's,[16] which correspond to freely precessing coherence between the ground state and an electronically excited state. In contrast, the signals in which we are interested represent coherences between Zeeman substates of the electronic ground state that precess at frequencies in the rf range and evolve on a time scale of the order of microseconds to milliseconds, much longer than that of typical optical FID's.

5. CONCLUSIONS

In summary, we have reported experimental investigations of the dynamics of the spin system in an atomic

ground state after an optical pumping process. The main emphasis of our study was on the measurement of the amplitude and the phase of the resulting FID as a function of laser intensity, optical detuning, and magnetic field strength. All experiments were performed with long excitation pulses, allowing the system to reach a steady state before the pulse was turned off to permit observation of the FID. Our theoretical and experimental results show that optically induced FID signals can be generated that correspond to an almost complete polarization of the ground-state sublevels. The most important parameter for the description of this process is the ratio between the optical pumping rate and the frequency at which the sublevel coherence evolves. At low pumping rates the FID amplitude is essentially proportional to the pumping rate; if the pumping rate exceeds the frequency corresponding to the sublevel splitting, the system becomes fully polarized, and the FID signal saturates. As the laser intensity is increased, the phase of the FID signal changes by some 90°. If the laser frequency is tuned away from resonance, the decrease of the optical pumping rate leads to smaller FID signals. The phase, however, is essentially independent of the optical detuning.

A simple model based on a Bloch-type equation was used to describe the dynamics of the ground-state spin polarization. Although the level scheme of sodium is more complicated than the $J = 1/2$ to $J' = 1/2$ system assumed for our model calculation, the agreement between theoretical predictions and experimental data is quite satisfactory. The simplicity of the model has the advantage of permitting an easy visualization of the dynamics, since the density operator of the system can be fully parameterized in a three-dimensional space.

It is clear that our results apply directly only to the spin dynamics of an atomic ground state. However, the fact that the amplitude and the phase of the FID depend strongly on the experimental parameters of the preparation stage may also be important for transient sublevel studies in optically excited states such as quantum-beat experiments. Since the effects reported here require that the system be saturated, similar experiments on excited states will in general require much higher laser intensities.

ACKNOWLEDGMENTS

This study was supported by the Schweizerischer Nationalfonds.

*Permanent address, Institut für angewandte Physik, Universität Münster, D-4400 Münster, Federal Republic of Germany.

REFERENCES

1. See, e.g., S. Haroche, "Quantum beats and time-resolved fluorescence spectroscopy," in *High Resolution Laser Spectroscopy*, K. Shimoda, ed. (Springer-Verlag, 1976), pp. 253–313, and references therein.
2. M. P. Silverman, S. Haroche, and M. Gross, "General theory of laser-induced quantum beats. I. Saturation effects of single laser excitation," Phys. Rev. A **18,** 1507–1516 (1978).
3. J. Mlynek and W. Lange, "A simple method of observing coherent ground state transients," Opt. Commun. **30,** 337–340 (1979).
4. R. M. Shelby, A. C. Tropper, R. T. Harley, and R. M. Macfarlane, "Measurement of the hyperfine structure of Pr^{3+}:YAG by quantum-beat free induction decay, hole burning, and optically detected nuclear quadrupole resonance," Opt. Lett. **8,** 304–306 (1983).
5. T. Kohmoto, Y. Fukuda, M. Tanigawa, T. Mishina, and T. Hashi, "Quantum beat free induction decay in Tm^{2+}:SrF_2: Fourier transform ESR spectroscopy by optical means," Phys. Rev. B **28,** 2869–2872 (1983).
6. See, e.g., M. S. Feld, M. M. Burns, T. U. Kühl, and P. G. Pappas, "Laser-saturation spectroscopy with optical pumpings," Opt. Lett. **5,** 79–81 (1980).
7. E. L. Hahn, "Nuclear Induction due to free Larmor precession," Phys. Rev. **77,** 297–298 (1950).
8. For a preliminary report see, e.g., S. Burschka and J. Mlynek, "Optically induced spin transients in the ground state of atomic sodium," Opt. Commun. **66,** 59–64 (1988).
9. See, e.g., A. Kastler, "Optical methods for studying Hertzian resonances," Science **158,** 214–221 (1967), and references therein.
10. See, e.g., T. Mishina, Y. Fukuda, and T. Hashi, "Optical generation and detection of $\Delta m = 2$ Zeeman coherence in the Cs ground state with a diode laser," Opt. Commun. **66,** 25–30 (1988).
11. F. Mitschke, R. Deserno, W. Lange, and J. Mlynek, "Magnetically induced optical self-pulsing in a nonlinear resonator," Phys. Rev. A **33,** 3219–3231 (1986).
12. D. Suter, M. Rosatzin, and J. Mlynek, "Optically driven spin nutations in the ground state of atomic sodium," Phys. Rev. A **41,** 1634–1644 (1990).
13. C. Cohen-Tannoudji and J. Dupont-Roc, "Experimental study of Zeeman light shifts in weak magnetic fields," Phys. Rev. A **5,** 968–984 (1972).
14. H. Lundberg and S. Svanberg, "Two quantum beat phenomena observed for magnetically tuned atomic sublevels," Opt. Commun. **27,** 235–238 (1978).
15. See, e.g., R. R. Ernst, G. Bodenhausen, and A. Wokaun, *Principles of Nuclear Magnetic Resonance in One and Two Dimensions* (Oxford U. Press, Oxford, 1987), pp. 119 ff.
16. See, e.g., R. G. Brewer, "Coherent optical transients," Phys. Today **30**(5), 50–59 (1977), and references therein.